





Non-conservative nature of boron in Arctic marginal ice zones

Penny Vlahos¹  , Kitack Lee² , Chang-Ho Lee², Lauren Barrett¹ & Lauren Juranek³

The Arctic Ocean is experiencing a net loss of sea ice. Ice-free Septembers are predicted by 2050 with intensified seasonal melt and freshening. Accurate carbon dioxide uptake estimates rely on meticulous assessments of carbonate parameters including total alkalinity. The third largest contributor to oceanic alkalinity is boron (as borate ions). Boron has been shown to be conservative in open ocean systems, and the boron to salinity ratio (boron/salinity) is therefore used to account for boron alkalinity in lieu of in situ boron measurements. Here we report this ratio in the marginal ice zone of the Bering and Chukchi seas during late spring of 2021. We find considerable variation in boron/salinity values in ice cores and brine, representing either excesses or deficits of boron relative to salinity. This variability should be considered when accounting for borate contributions to total alkalinity (up to $10 \mu\text{mol kg}^{-1}$) in low salinity melt regions.

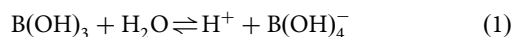
¹Department of Marine Sciences, University of Connecticut, Groton, CT, USA. ²Division of Environmental Science and Technology, Pohang University of Science and Technology, Pohang, Korea. ³College of Earth, Ocean, and Atmospheric Sciences, Oregon State University, Corvallis, OR, USA.
email: penny.vlahos@uconn.edu

The Arctic Ocean is undergoing rapid change. Summer areal sea-ice extent has been steadily decreasing, reaching a low of 3.41 million km² in 2012, equivalent to 48.5% less than the mean for the period 1979–2000¹. It is predicted that the Arctic will have ice-free Septembers before 2050, and consequently it is expected that the receding and thinning permanent sea-ice cap will be replaced by seasonal annual ice^{2,3}. Several biogeochemical processes are coupled to these shifts, including increased surface water productivity because of less light limitation⁴; increased CO₂ drawdown from enhanced productivity in some regions⁵ and increased air-sea gas exchange, leading to increased acidification⁶; and changes in hydrodynamics because of the removal of a permanent ice cap⁷. As the Arctic shifts to a system dominated by annual ice, the complete seasonal melt will lead to intensified seasonal freshening of Arctic surface waters in ice melt zones. The impact on Arctic Ocean biogeochemistry remains unclear.

Although the Arctic represents only 3% (14.06 million km²) of the global sea surface area, it accounts for 10% of the global ocean carbon uptake^{8,9}. A major concern for future predictions is the impact these changes in sea ice extent will have on the Arctic as a sink for rising atmospheric CO₂ levels. The influence of intensifying annual ice melt processes on carbonate system parameters is not well understood.

Atmospheric CO₂ uptake is impacted by processes altering the differences in partial pressure of CO₂ (pCO₂) across the air-sea boundary. The pCO₂ in surface waters is dependent on a cascade of carbonate system reactions and the resulting buffering capacity of the waters. Carbonate system variables including pH, dissolved inorganic carbon (DIC), and total alkalinity (A_T) are used in combination to define the CO₂ chemistry of a water parcel. To isolate bicarbonate and carbonate contributions, most carbonate system studies use well-established ratios and parameterizations to correct for other constituents that may add to A_T¹⁰. Boron in the form of borate (orthoborate) ions (B(OH)₄⁻) is the third greatest contributor to A_T in marine systems after bicarbonate and carbonate.

Boron (B) is ubiquitous in the environment, occurring naturally in more than 80 minerals. It is a major element in seawater at concentrations in the mg kg⁻¹ range. Because of the low dissociation constant of B in seawater, the majority of marine B is found in the form of boric acid, B(OH)₃, although approximately 20% of this is ionized to borate. The exchange between boric acid and borate is described by its equilibrium reaction (1), which is used to determine the contribution of borate to seawater alkalinity (the capacity of water to resist a change in pH or acidification):



In seawater B is a conservative element, and the boron to salinity ratio (B/S) has been shown to be uniformly consistent across ocean waters (North Atlantic and North Pacific) at salinities of 33–36 g kg⁻¹ (0.1336 ± 0.0005 mg kg⁻¹ ‰⁻¹)¹¹. The B/S ratio is known to shift in some coastal regions including the Baltic Sea¹², and in low salinity waters where variations in freshwater endmember B concentrations may become important¹³. As the Arctic receives 11% of total riverine inputs to the global ocean but represents only 1.4% of the ocean volume¹⁴, it too undergoes considerable freshening. Olafsson et al.¹⁵ reported a B/S ratio of 0.1324 ± 0.0008 mg kg⁻¹ ‰⁻¹ in the eastern Arctic in water having salinities as low as 30 g kg⁻¹, and found that the B/S ratio, though slightly lower, was reasonably consistent with that of open ocean values. However, there are additional sources of freshwater from sea ice melt that contribute to Arctic freshening, and the B/S ratio in these sources is highly uncertain. There is little known about the B/S ratio in low salinity (<30 g kg⁻¹) marginal ice zones

(MIZs), though this is critical to our ability to quantify A_T when predicting future CO₂ uptake in Arctic waters. Here we present results of analysis of B/S ratios in 100 samples collected between 20 May and 12 June 2021 along the MIZ of the Bering and Chukchi Seas, in a study to evaluate the B/S ratio in these dynamic, low salinity regions.

Results and discussion

Boron in open ocean water: Samples were collected in a northerly direction along a transect across the Bering Sea (stations 1–4) into the Chukchi Sea MIZ (stations 5–9), and then in a southerly direction along the same transect (stations 10–16) (see Supplementary Table 1). Total B concentrations were measured in open ocean, ice core, and brine (the interstitial water of the sea ice matrix) samples. Figure 1a, b shows the total B concentration and B/S for surface water samples (1–2 m) across the transects. Total B ranged from 3.7 to 4.4 mg kg⁻¹ and the B/S ratios ranged from 0.1280 to 0.1330. Notably, a region of relatively low B

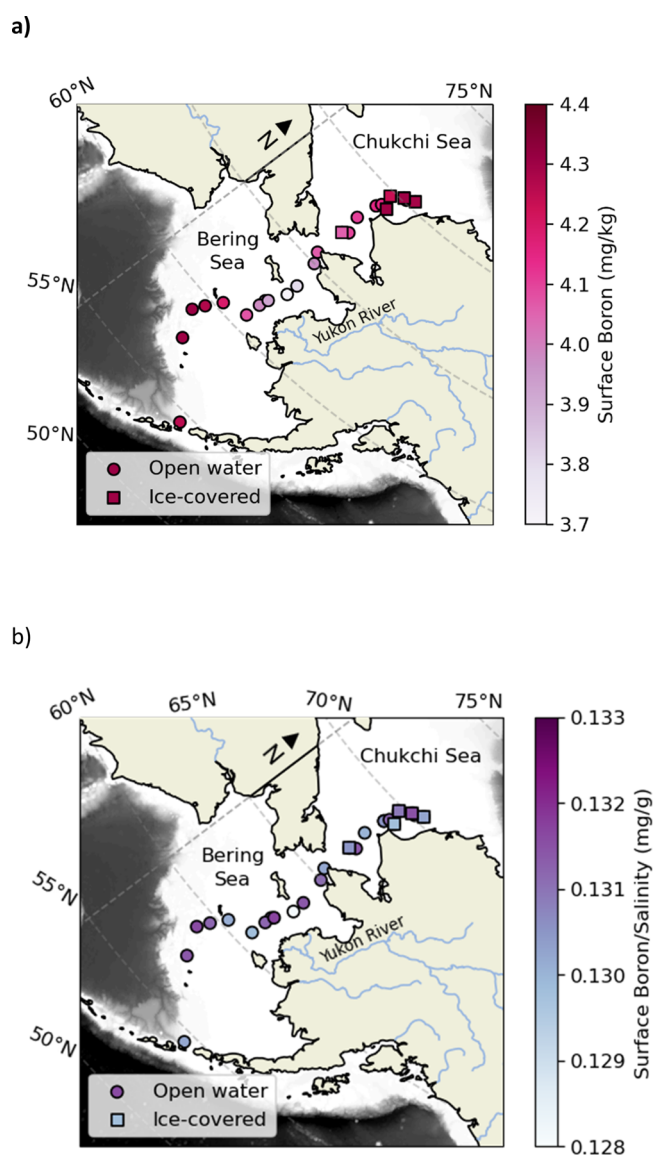


Fig. 1 Station location on the RV Sikuliaq between May 20th to June 14th, 2021. Ice covered stations are depicted with square markers and open water stations are represented in round markers. **a** Boron concentrations in surface water samples across transect in mg kg⁻¹ and **b** boron to salinity ratios for all surface water stations.

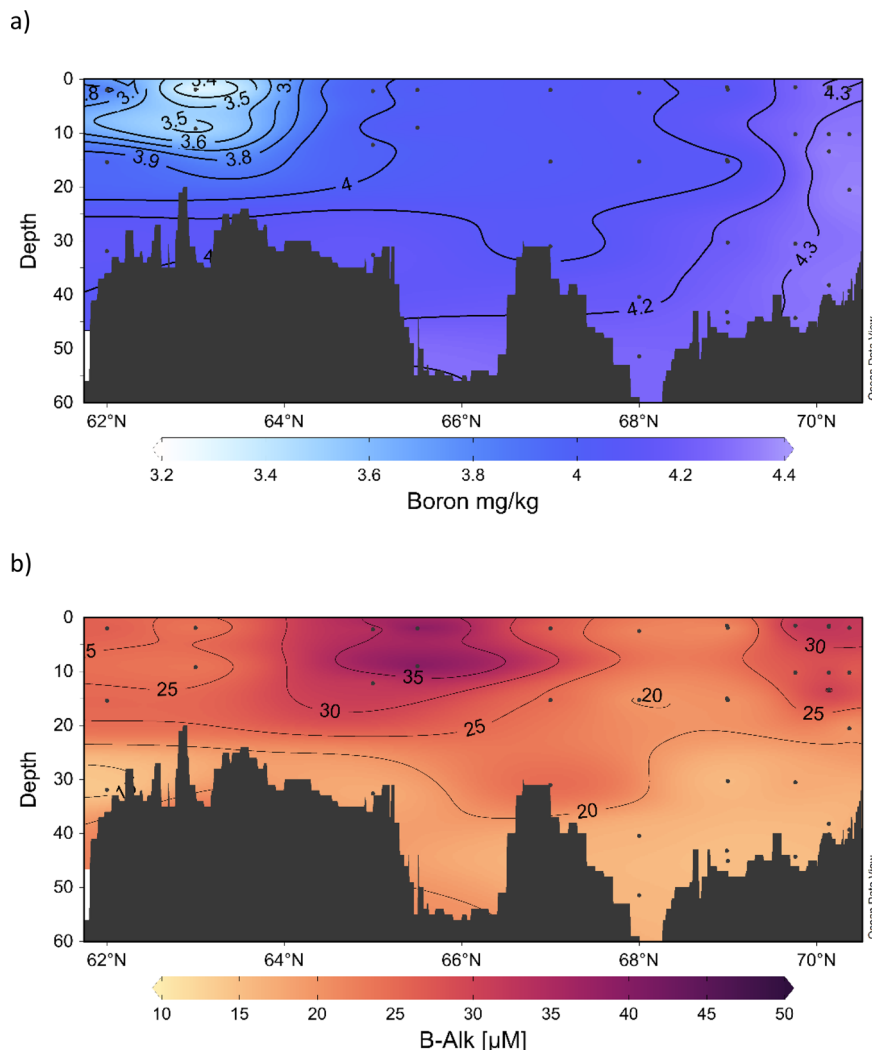


Fig. 2 Depth profiles. **a** Total boron concentrations in mg kg^{-1} and **b** alkalinity due to borate (B-Alk) in $\mu\text{mol kg}^{-1}$.

concentration and B/S ratio occurred in ice-free waters having substantial freshening associated with the Yukon–Kuskokwim River plume. This was associated with characteristically higher temperatures (4°C) and lower salinities (28 g kg^{-1}) at this station. The low values of this region were also apparent in the depth profiles of total B and borate (Fig. 2a, b).

Lower water temperatures and lower salinities tend to increase the pK_a in Eq. (1)¹⁶, thus decreasing the proportion of borate ions. The resulting acidity constants for the boric acid/borate acid-base pair ranged from 8.844 to 8.951, and borate ranged from 3–14 % of total boron. The total borate contribution to A_T ranged from $11 \mu\text{mol kg}^{-1}$ in the lower pH waters ($\text{pH} = 7.300$, $A_T = 2297 \mu\text{mol kg}^{-1}$) and up to $57 \mu\text{mol kg}^{-1}$ in the relatively alkaline waters ($\text{pH} = 8.096$, $A_T = 2085 \mu\text{mol kg}^{-1}$).

Boron in Snow: Supplementary Fig. 1 identifies locations of snow and ice stations (5,6,8,9 and 12). Snow samples across all ice stations ($n = 4$) were consistently low in B, with concentrations that were either below the detection limit or $<0.151 \text{ mg kg}^{-1}$, and all had zero salinity values. These B values are within the range reported for a various snow sample types ($0\text{--}0.32 \text{ mg kg}^{-1}$, $n = 79$)¹⁷ in regions of North America that are less remote than the Arctic and may be a useful reference endmember in Arctic atmospheric wet deposition.

Boron in Ice Cores and Brine: Fig. 3 shows the total B in ice cores and brine for the five ice stations in this study. All stations

had a general trend of increasing total B with depth. The B/S ratios at stations 5 and 6 remained consistent across depth and between ice and brine, but were slightly lower than those reported for open ocean samples^{11,16}. Samples from these stations were obtained during the northward sampling along the transect. Samples from stations 8 and 9 were obtained during the southward sampling along the transect and had B/S ratios that were much less consistent. Fig. S1 shows the location of the ice sheet before and during sampling at each station. On 2 May the ice sheet was still attached to the Alaskan coast, but by 9 May it had detached and moved westward. The ice sheet underwent a flow reversal, and therefore the location of the stations in our study were subject to a short period of no ice cover before the sheet returned. Station 5 was the earliest ice station, furthest into the ice sheet relative to the ice edge and was likely the least disturbed station in terms of interactions with open ocean water and advancement of melt. The subsequent stations were closer to the ice edge and the results obtained for these may reflect the mechanical impacts of the MIZ movements.

It is not clear why the B/S ratios at stations 8 and 9 were higher (50%) or lower (25%) than the established open ocean ratio of 0.1336, although likely mechanisms are suggested from other studies. As seawater freezes, many of the salts are rejected. However, within the ice crystals that form, selected cations (i.e., Ca^{2+}) tend to concentrate in the liquid regions (brine channels)

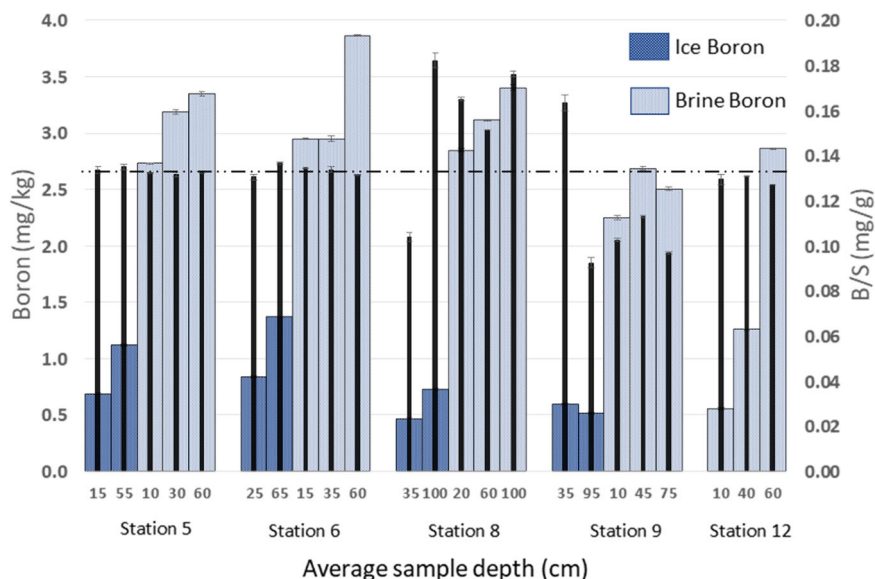


Fig. 3 Vertical profiles of total boron and boron to salinity ratios (B/S) across all five ice stations. Wide bars represent total boron in ice (dark blue) and brine (light blue) and thin, solid bars (black) represent the B/S ratios. The horizontal dashed line represents the open ocean B/S ratio from Lee et al.¹¹. Error bars represent uncertainty in replicate measurements ($n = 3$).

between the crystals^{18,19}. As these ions accumulate to levels at which solubility limits are reached, calcium carbonate minerals begin to precipitate inorganically²⁰. In these unique micro-environments, B may concurrently precipitate with CaCO_3 in the brine channels²¹. The ice conditions resulting in the inorganic precipitation of CaCO_3 in conjunction with B are unknown, but we hypothesize that such inorganic processes (precipitation, re-dissolution) may have occurred at stations 8 and 9. In addition, there are several shifts in brine channel chemistry associated with upward and downward flushing of the brine network, changes associated with the porosity of the brine and coalescence of brine networks during melt^{22,23}.

The B/S ratios in the sampled ice cores and brine ($n = 19$) averaged 0.1333 ± 0.0231 . Surprisingly, this is similar to the open ocean B/S ratio, although with a much larger range. The average and range suggest a decoupling of B from the salinity matrix from which it is derived during the evolution of the brine network. This has important implications for the determination of the B contribution to alkalinity in melt regions, and implies that for studies where highly resolved alkalinity contributions are required ($\pm 2 \mu\text{M}$), either direct B measurements should be made or greater uncertainty should be incorporated into estimates of borate contributions to A_T . This becomes important for melt waters where the salinity is $< 30 \text{ g kg}^{-1}$ and very important for ice and brine studies.

Boron to Salinity Ratios: Fig. 4a, b shows the B/S ratios across all sample types. There were discernable differences between the open ocean B/S ratio of 0.1336^{11,16} and our mean open ocean value of 0.1305 ± 0.0008 (Fig. 4c). The difference can lead to as much as about $9 \mu\text{mol kg}^{-1}$ of total boron concentration. This translates to a difference of only $2 \mu\text{mol kg}^{-1}$ in total alkalinity. Nevertheless, it is important that investigators are aware of these uncertainties in future carbonate system studies. Comparison of B measurements in this study with those derived using the open ocean B/S ratios resulted in total B uncertainties of 0–21 μM B for ice cores and 0.4–87 μM B for brine samples. The resulting uncertainty in borate alkalinity (assuming borate is $< 12\%$ of total boron) is 0–10 μM . Such variations in carbonate system calculations conducted in MIZ regions could be substantial, and this warrants further investigation. In this study, the overall B/S ratio in the MIZ across this large range of salinities (see Fig. 4a, b) was

$0.1312 \pm 0.0008 \text{ mg (kg } \%)^{-1}$ and in ice and brine alone was $0.1333 \pm 0.02313 \text{ mg (kg } \%)^{-1}$.

This study showed important shifts in B/S ratios in the Arctic MIZ, which is critical information for future A_T interpretations and ultimately CO_2 uptake studies in ice melt environments. The shifts may lead to inaccuracies in carbonate system analyses of between 0 and $2 \mu\text{mol kg}^{-1}$ in open melt waters (salinities $28\text{--}34 \text{ g kg}^{-1}$) or between 0 and $10 \mu\text{mol kg}^{-1}$ in ice and brine. All the ice and brine samples in this study were derived from annual ice of a single ice sheet. Consequently, it is important that this work be expanded to include: (i) annual ice across Arctic regions; (ii) annual ice during summer as melt progresses; and (iii) multi-year ice profiles, to ascertain the impact they may have as they progressively thin and add to Arctic water chemistry. This evidence for the non-conservative behavior of B in ice and brine has not previously been documented in the microenvironments within the sea ice. The observed non-conservative nature of B that we have observed in some ice samples and the impacts of our observations on air-sea CO_2 flux and carbonate calculations in open waters with some meltwater is likely small. However, as these systems are currently not well understood and melt intensification is inevitable, we strongly believe that such non-conservative patterns during ice formation and melting are highly noteworthy.

Methods

Sample collection. All samples for B were collected in 100 mL polycarbonate bottles. Open water samples were collected using rosette casts and Teflon-lined Niskin bottles (15 stations). The remaining samples were collected at five ice stations (See details in Supplementary Table 2). Snow samples were collected during on-ice sampling from clearly loose surface snow that lay above the ice sheet. Brine samples were collected by drilling with an Eskimo 10 inch HC40 ice auger to the desired depth within the ice and then allowing brines from the surrounding ice to drain into the hole ($< 5 \text{ min}$). Brine was collected using a submersible sump pump through tubing placed in the sack hole. Ice cores were collected using a Kovacs Mark II coring system, which retrieved a 9-cm diameter ice core that was sectioned into 10-cm subsections while on the ice. Under ice water was collected once the core was removed and pumped into 5 L compressible LDPE Exetainers.

Total Boron. Boron samples were shipped to Kitack Lee at Pohang University of Science and Technology, Korea. Samples were analyzed using the four-step curcumin method by Upstrom²⁴ as refined by Liu and Lee²⁵. The results indicated considerably better precision and accuracy for B concentration measurements than

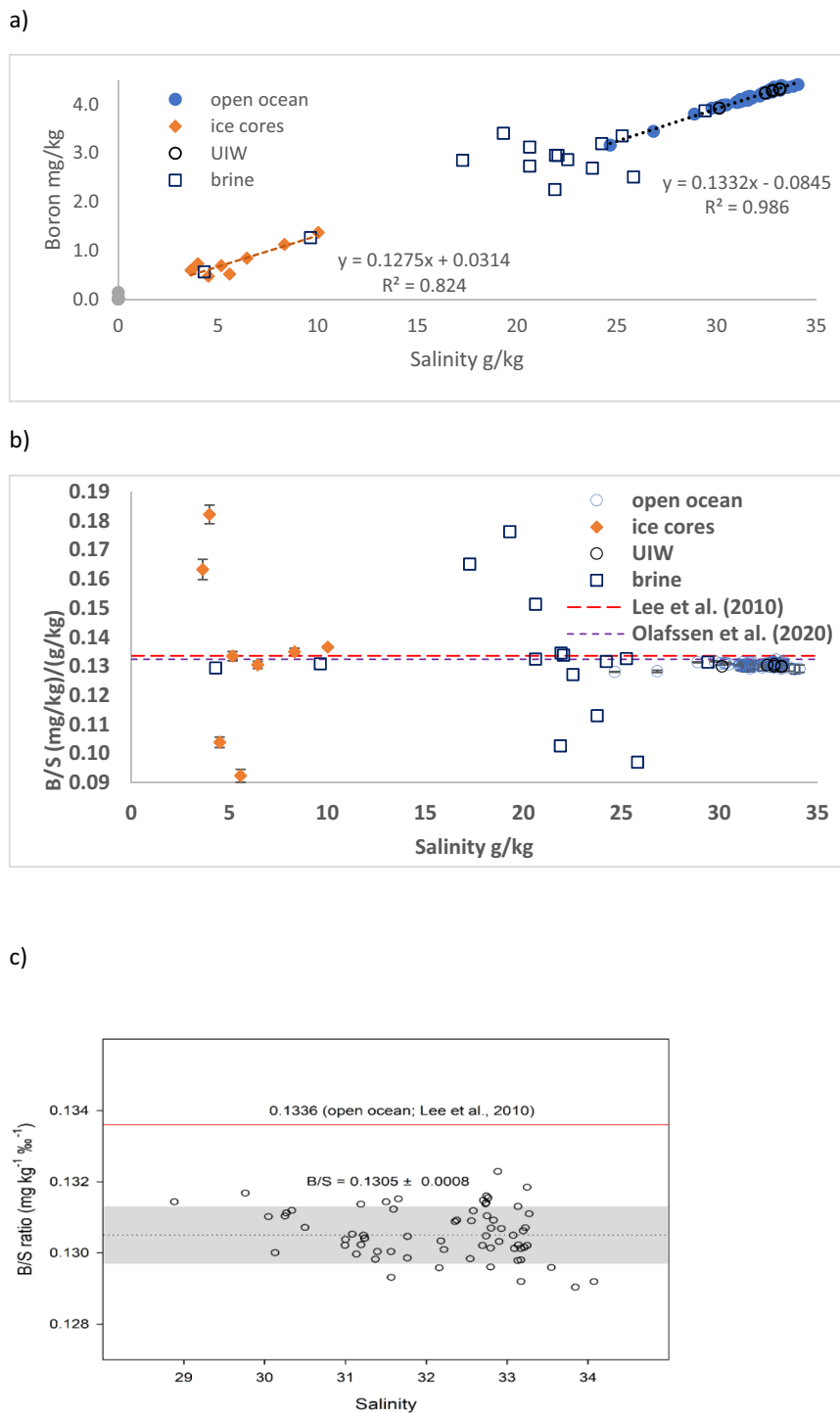


Fig. 4 Variation in the boron to salinity ratios (B/S) across all sample types. Values are shown relative to the established values of Lee et al.¹¹ for 5 open ocean regions and Olafsson et al.¹⁵ in the North Atlantic and polar regions: **(a)** Total B (all samples from this study) versus salinity, **(b)** B/S ratio (all samples from this study) versus salinity, and **(c)** B/S ratio in open seawater samples from this study versus salinity where the gray shaded area represents 1 standard deviation.

both the conventional curcumin method and other analytical techniques (Supplementary Fig. 2 and Supplementary Table 3). Briefly, water samples were collected in three 100 mL polyethylene bottles and placed in a water bath at 25 °C. A 500 µL aliquot of sample was pipetted into a reaction bottle along with 1.0 mL of glacial acetic acid and 3.0 mL of propionic acid anhydride, followed by the dropwise addition of 250 µL of oxalyl chloride. After the mixture had equilibrated at room temperature (20 min), 3.0 mL of a sulfuric–acetic acid mixture and 3.0 mL of curcumin reagent were added to the reaction bottle, and the solution was mixed, and reacted to completion (70 min). During the reaction time an orange-colored boron–curcumin complex (rosocyanine) formed. For analysis of low S samples, the

amounts of sample and reagents were increased; 1000 µL for sample, 2.0 mL for glacial acetic acid, 5.0 mL for propionic anhydride, 500 µL for oxalyl chloride, and 4.0 mL for a sulfuric–acetic acid and curcumin reagent²⁶. The absorbance of the final solution was measured at 543 nm using a 1 cm quartz cell and corrected for the absorbance of reagent blanks (%RSD range 0.3–0.7%).

Salinity. Salinity (Practical Salinity Scale) was measured onboard in accordance with IOC, SCOR and IAPSO²⁷, using a Portasal Salinometer 8410A. The

instrument was calibrated at 25 °C against IAPSO standard seawater. The precision was at least $\pm 0.002 \text{ g kg}^{-1}$.

pH. The concentration of hydrogen ion (pH) was determined spectrophotometrically using an Agilent Cary 60 UV-Vis systems spectrophotometer and m-cresol purple indicator dye following Carter et al.²⁸. 40 ml samples were temperature equilibrated in the instrument's thermostatted cell holder at 25 °C and precision and accuracy monitored throughout the cruise using triplicate samples from the same Niskin bottle and TRIS buffers. The precision of the pH measurements is estimated to be approximately ± 0.0014 ²⁹. Further details on the methods and quality control are described in Millero et al.³⁰ and Woosley et al.²⁹. All open water samples and under ice water were analyzed for pH. Brine and ice samples were not included in the analysis due to limited sample availability.

Borate. Acidity constants for boric acid/borate equilibria were calculated after Dickson¹⁶ using the temperature and salinity of each discrete sample (Supplementary Table 1). Note borate alkalinity for ice and brine could only be estimated due to the lack of accurate pH profile data and is therefore not used in this analysis.

Reporting summary. Further information on research design is available in the Nature Research Reporting Summary linked to this article.

Data availability

All data and metadata relevant to this study are available through the U.S National Science Foundation Arctic Data Center. urn:uuid:ed43726c-fbae-4eb0-89fe-2e0d69f60f55. Data is also available directly through our project website <https://env.chem.uconn.edu/arctic-amiza/>.

Received: 21 March 2022; Accepted: 7 September 2022;

Published online: 19 September 2022

References

- Liu, J., Song, M., Horton, H. M. & Hu, Y. Reducing spread in climate model projections of a September ice-free Arctic. *Proc. Natl Acad. Sci.* **110**, 12571–12576 (2013).
- Vinnikov, K. Y. et al. Global warming and northern hemisphere sea ice extent. *Science* **286**, 1934–1937 (1999).
- Wang, B., Zhou, X., Ding, Q. & Liu, J. Increasing confidence in projecting the Arctic ice-free year with emergent constraints. *Environ. Res. Lett.* **16**, 094016 (2021).
- Achim, R. et al. Pan-arctic ocean primary production constrained by turbulent nitrate fluxes. *Front. Mar. Sci.* **7**. <https://doi.org/10.3389/fmars.2020.00150> (2020).
- Lewis, K. M., van Dijken, G. L. & Arrigo, K. R. Changes in phytoplankton concentration now drive increased Arctic Ocean primary production. *Science* **369**, 198–202 (2020).
- Qi, D. et al. Rapid acidification of the Arctic Chukchi Sea waters driven by anthropogenic forcing and biological carbon recycling. *Geophys. Res. Letters* **49**, e2021GL097246 (2022).
- Woodgate, R. A. Increases in the Pacific inflow to the Arctic from 1990 to 2015, and insights into seasonal trends and driving mechanisms from year-round Bering Strait mooring data. *Prog. Oceanogr.* **160**, 124–154 (2017).
- Bates, N. R. & Mathis, J. T. The Arctic Ocean marine carbon cycle: evaluation of air-sea CO₂ exchanges, ocean acidification impacts and potential feedbacks. *Biogeosciences* **6**, 2433–2459 (2009).
- Yasunaka, S. et al. Mapping of the air-sea CO₂ flux in the Arctic Ocean and its adjacent seas: Basin-wide distribution and seasonal to interannual variability. *Polar Sci.* **10**, 323–334 (2016).
- Orr, J., Epitalon, J.-M., Dickson, A. G. & Gattusode, J.-P. Routine uncertainty propagation for the marine carbon dioxide system. *Mar. Chem.* **207**, 84–107 (2018).
- Lee, K. et al. The universal ratio of boron to chlorinity for the North Pacific and North Atlantic oceans. *Geochim. Cosmochim. Acta* **74**, 1801–1811 (2010).
- Kuliński, K., Szymczycha, B., Koziarowska, K., Hammer, K. & Schneider, B. Anomaly of total boron concentration in the brackish waters of the Baltic Sea and its consequence for the CO₂ system calculations. *Mar. Chem.* **204**, 11–19 (2018).
- Lee, K., Lee, C. H., Lee, J. H., Han, I. S. & Kim, M. Deviation of boron concentration from predictions using salinity in coastal environments. *Geophys. Res. Lett.* **46**, 4809–4815 (2019).
- Eakins, B. W. & Sharman, G. F. *Volumes of the World's Oceans from ETOPO1* (NOAA National Geophysical Data Center, 2010).
- Olafsson, J. et al. Boron to salinity ratios for Atlantic, Arctic and Polar Waters: a view from downstream. *Mar. Chem.* **224**, 103809 (2020).
- Dickson, A. G. Thermodynamics of the dissociation of boric acid in synthetic seawater from 273.15 to 318.15 K. *Deep-Sea Res.* **37**, 755–766 (1990).
- Feth, J. H., Rogers, S. M. & Robertson, C. E. Chemical composition of snow in the Northern Sierra Nevada and other areas. Geological Survey Water-supply Paper 1535-J, Washington, D.C. 20402 (1964).
- Obbard, R. W. et al. Synchrotron X-ray fluorescence spectroscopy of salts in natural sea ice. *Earth Space Sci.* **3**, 463–479 (2016).
- Kim, K., Choi, W., Hoffmann, M. R., Yoon, H.-I. & Park, B.-K. Photoreductive dissolution of iron oxides trapped in ice and its environmental implications. *Environ. Sci. Technol.* **44**, 4142–4148 (2010).
- Dieckmann, G. S. et al. Calcium carbonate as ikaite crystals in Antarctic sea ice. *Geophys. Res. Lett.* **35**, L08501 (2008).
- Kobayashi, K., Hashimoto, Y. & Wang, S.-L. Boron incorporation into precipitated calcium carbonates affected by aqueous pH and boron concentration. *J. Hazard. Mater.* **383**, 121183 (2020).
- Golden, K. M., Ackley, S. F. & Lytle, V. I. The percolation phase transition in sea ice. *Science* **282**, 2238–2241 (1998).
- Perovich, D. K. & Gow, A. J. A quantitative description of sea ice inclusions. *J. Geophys. Res.* **101**, 18327–18343 (1996).
- Uppström, L. R. The boron/chlorinity ratio of deep-sea water from the Pacific Ocean. *Deep-Sea Res.* **21**, 161–162 (1974).
- Liu, Y. M. & Lee, K. Modifications of the curcumin method enabling precise and accurate measurement of seawater boron concentration. *Mar. Chem.* **115**, 110–117 (2009).
- Uppström, L. R. A modified method for determination of boron with curcumin and a simplified water elimination procedure. *Anal. Chim. Acta* **43**, 475–486 (1968).
- IOC, SCOR and IAPSO. The international thermodynamic equation of seawater—2010: Calculation and use of thermodynamic properties. Intergovernmental Oceanographic Commission, Manuals and Guides No. 56, UNESCO (English), 196pp. (2010).
- Carter, B. R., Radich, J. A., Doyle, H. L. & Dockson, A. G. 2013. An automated system for spectrophotometric seawater pH measurements. *Limnol. Oceanogr. Methods* **11**, 1 (2013).
- Woosley, R. J., Millero, F. J. & Takahashi, T. Internal consistency of the inorganic carbon system in the Arctic Ocean. *Limnol. Oceanogr. Methods* **15**, 887–896 (2017).
- Millero, F. J., Woosley, R. J., Margolin, A. R. & Huang, F. *Global Ocean Repeat Hydrography Study: pH, Total Alkalinity, and Total CO₂ measurements in the Arctic Ocean* (CDIAC, Oak Ridge National Laboratory, 2016).

Acknowledgements

The authors would like to thank Chief Scientist Dr. Robert Mason and the captain and crew of the RV Sikuliaq for excellent logistical support, and Steve Roberts for processing satellite ice imagery. This work was supported by the U.S. National Science Foundation (NSF) Office of Polar Programs Award #1630846. Kitack Lee was supported by National Research Foundation of Korea (NRF-2021R1A2C3008748).

Author contributions

P.V. proposed the project, was PI on the funded project, performed field work, data analyses and wrote the manuscript. K.L. supervised laboratory analysis of boron, performed data analyses and contributed to this manuscript. C.B. performed laboratory analyses, data analyses and contributed to this manuscript. L.B. performed field work, laboratory and data analyses and contributed to this manuscript. L.J. performed field ice coring and sampling, provided the subsamples to be analyzed and details on ice core temperatures and depths.

Competing interests

The authors declare no competing interests.

Additional information

Supplementary information The online version contains supplementary material available at <https://doi.org/10.1038/s43247-022-00552-0>.

Correspondence and requests for materials should be addressed to Penny Vlahos.

Peer review information *Communications Earth & Environment* thanks the anonymous reviewers for their contribution to the peer review of this work. Primary Handling Editors: Olivier Sulpis and Clare Davis.

Reprints and permission information is available at <http://www.nature.com/reprints>

Publisher's note Springer Nature remains neutral with regard to jurisdictional claims in published maps and institutional affiliations.



Open Access This article is licensed under a Creative Commons Attribution 4.0 International License, which permits use, sharing, adaptation, distribution and reproduction in any medium or format, as long as you give appropriate credit to the original author(s) and the source, provide a link to the Creative Commons license, and indicate if changes were made. The images or other third party material in this article are included in the article's Creative Commons license, unless indicated otherwise in a credit line to the material. If material is not included in the article's Creative Commons license and your intended use is not permitted by statutory regulation or exceeds the permitted use, you will need to obtain permission directly from the copyright holder. To view a copy of this license, visit <http://creativecommons.org/licenses/by/4.0/>.

© The Author(s) 2022